Eur Biophys J (2000) 29: 439–454

ARTICLE

Mafalda Nina · Simon Bernèche · Benoît Roux

Anchoring of a monotopic membrane protein: the binding of prostaglandin H_2 synthase-1 to the surface of a phospholipid bilayer

Received: 20 December 1999 / Revised version: 26 March 2000 / Accepted: 26 March 2000

Abstract Prostaglandin H_2 synthases (PGHS-1 and -2) are monotopic peripheral membrane proteins that catalyse the synthesis of prostaglandins in the arachidonate cascade. Picot et al. (1994) proposed that the enzyme is anchored to one leaflet of the bilayer by a membrane anchoring domain consisting of a right-handed spiral of amphipathic helices (residues 73–116) forming a planar motif. Two different computational approaches are used to examine the association of the PGHS-1 membrane anchoring domain with a membrane via the proposed mechanism. The electrostatic contribution to the free energy of solvation is obtained by solving numerically the finite-difference Poisson equation for the protein attached to a membrane represented as a planar slab of low dielectric. The nonpolar cavity formation and van der Waals contributions to the solvation free energy are assumed to be proportional to the water accessible surface area. Based on the optimum position determined from the continuum solvent model, two atomic models of the PGHS-1 anchoring domain associated with an explicit dimyristoylphosphatidylcholine (DMPC) bilayer differing by the thickness of the membrane bilayer were constructed. A total of 2 ns molecular dynamics simulation were performed to study the details of lipid-protein interactions at the microscopic level. In the simulations the lipid hydrocarbon chains interacting with the anchoring domain assume various shapes, suggesting that the plasticity of the membrane is significant. The hydrophobic residues in the membrane side of the helices interact with the hydrophobic membrane core, while the positively charged residues interact with the lipid polar headgroups to stabilize the anchoring of the membrane domain to the upper half of the bilayer. The phosphate headgroup of one DMPC molecule disposed at the center of the spiral formed by helices A, B, C and D interacts strongly with Arg120, a residue on helix D that has previously been identified as being important in the activity of PGHS-1. In the full enzyme structure, this position corresponds to the entrance of a long hydrophobic channel leading to the cyclooxygenase active site. These observations provide insights into the association of the arachidonic acid substrate to the cyclooxygenase active site of PGHS-1.

Key words Prostaglandin H_2 synthase-1 · Phospholipid membranes · Computer simulation · Poisson equation · Mean-field approximation

M. Nina[1] · S. Bernèche[2] · B. Roux (✉)[2]
Membrane Transport Research Group (GRTM),
Department of Chemistry, University of Montreal,
C.P. 6128, succ. A, Quebec H3C 3J7, Canada
e-mail: benoit.roux@umontreal.ca

Current addresses:
[1] Laboratoire de Biologie Structurale, I.G.B.M.C.,
4 Rue Laurent Fries, 67404 Illkirch Cedex, Strasbourg, France
[2] Department of Biochemistry and Structural Biology,
Weill Medical College of Cornell University,
New York, NY 10021, USA

Introduction

Prostaglandin H_2 synthases (PGHS) are *N*-glycosylated membrane proteins responsible for the synthesis of prostaglandins involved in important physiological processes such as smooth muscle contraction, inflammation, parturition and platelet aggregation (Otto et al. 1993; Smith et al. 1991). Two isoforms have been identified: PGHS-1 and PGHS-2, also referred as cyclooxygenase COX-1 and COX-2 (for reviews, see Hla et al. 1993; Loll and Garavito 1994). PGHS-1 is constitutively expressed in most tissues and is responsible for the physiological production of prostaglandins. PGHS-2 is induced by cytokines, mitogens and endotoxins in inflammatory cells, and is responsible for the elevated production of prostaglandins during inflammation. Prostaglandin H_2 synthases are located primarily in the endoplasmic reticulum (Smith and Marnett 1991) and possess two catalytic active sites to perform the synthesis of prostaglandin H_2 from arachidonic acid in two consecutive steps: a cyclooxygenase site that converts

arachidonic acid to PGG_2 and a hydroperoxydase site that reduces the hydroxyl group of PGG_2 to PGH_2 (Ohki et al. 1979; van der Ouderaa et al. 1977; Pagels et al. 1983). The first product, PGG_2 hydroperoxide, is converted into one of several prostanoid hormones. The cyclooxygenase activity of PGHS-1 and PGHS-2 is the target of an economically important class of drugs known as non-steroidal anti-inflammatory drugs (NSAIDs), which makes it one of the most interesting targets in the pharmaceutical industry (Holtzman et al. 1991; Meade et al. 1993). The primary mechanism of NSAIDs in the treatment of inflammation is the inhibition of the two isoforms of PGHS. Much recent effort has been made to produce selective inhibitors of PGHS-2 in the belief that these will lack the gastrointestinal damaging effects of traditional NSAIDs (McCartney et al. 1999). The three-dimensional structures of ovine 576-amino acid PGHS-1 complexed with the NSAID flurbiprofen (Picot et al. 1994), with 2-bromoacetoxybenzoic acid (a potent aspirin analogue) (Loll et al. 1995), as well as with iodinated indomethacin and suprofen (Loll et al. 1996), have been determined by X-ray crystallography. X-ray structures of unliganded murine PGHS-2 and complexed with flurbiprofen, indomethacin and a selective inhibitor (SC-558) have also been obtained (Kurumbail et al. 1996). The structure of human PGHS-2, determined in the presence of a selective inhibitor, is similar to that of PGHS-1 (Luong et al. 1996).

PGHS are classified as integral membrane proteins because detergents are required to extract the enzyme from the membrane (Smith and Marnett 1991). However, in contrast to many other membrane proteins such as the photosynthetic reaction center (Deisenhofer and Michel 1989), bacteriorhodopsin (Henderson et al. 1990), porins (Cowan et al. 1995) or the KcsA K^+ channel from *Streptomyces lividans* (Doyle et al. 1998), the crystal structure of PGHS-1 reveals no transmembrane motifs which could serve to anchor the protein to the lipid membrane (see Fig. 1) (Picot et al. 1994). Since it is unlikely that the native conformation is significantly affected by detergent extraction or crystallization, a novel and attractive model for membrane attachment was proposed by Picot et al. (1994) based on a close examination of the X-ray structure. According to this model, the dimer is anchored to one leaflet of the bilayer through the hydrophobic surface of a number of amphipathic helices, in a similar way that surface-active peptides bind to membranes with their nonpolar residues on the lower surfaces interacting with the hydrophobic interior of the bilayer (Kaiser and Kezdy 1987). The proposed membrane attachment motif consists of a right-handed spiral of amphipathic α-helices A, B, C and D (residues 73–116) lying approximately in a plane acting as a membrane anchoring domain (see Fig. 1). A corresponding motif on the adjacent monomer faces in the same direction. Helices A, B, C and the beginning of helix D are amphipathic and their hydrophobic surface faces outward away from the main body of the protein, forming a large hydrophobic patch on the exterior of the dimer (Fig. 2). The amphipathic helices A (residues 73–82), B (residues 86–92), C (residues 97–105) and the beginning of helix D (residues 108–116) contain hydrophobic residues such as alanines, valines, leucines, isoleucines and, interestingly, several aromatic residues, such as phenylalanines (4) and tryptophans (3). The opposite side of the helices contains polar and a few positively charged residues (mainly arginines) which could interact with the lipid polar headgroups. Based on the crystal structures of the PGHS-1 and PGHS-2, it was confirmed by experiments on chimeric proteins which did not contain the putative membrane anchoring domains that the amphipathic helices act as membrane anchors (Yi et al. 1998).

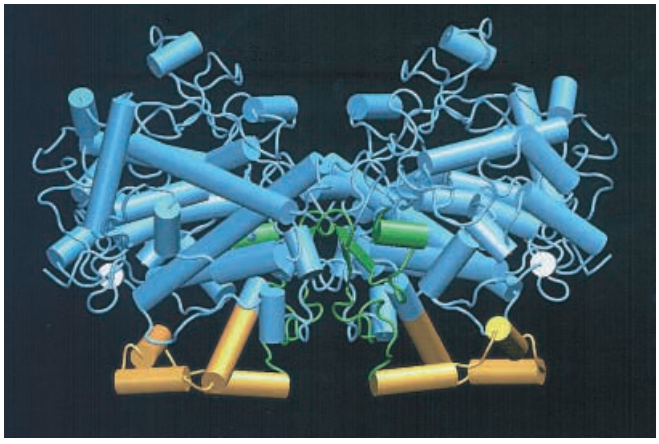

Fig. 1 PGHS-1 dimer viewed along the dimer interface with the molecular two-fold axis vertical (Picot et al. 1994). The catalytic domain, the EGF-like module and the anchoring domain are colored in *blue*, *green* and *orange*, respectively

Recent results by Spencer et al. (1999) provide direct support for the hypothesis that PGHS-1 is a monotopic membrane protein which associates with bilayers through the anchoring domain. Membrane-associated forms of ovine PGHS-1 and human PGHS-2 were labeled using a hydrophobic, photoactivable reagent, isolated, cleaved and the photolabeled peptides were sequenced. The results provide direct biochemical support for the hypothesis that PGHS-1 and -2 do associate with membranes through the monotopic anchoring domain. Furthermore, it was demonstrated, via site directed mutations, that the amphipathic character of each helix (A, B, and C) is important for the assembly and folding of ovine PGHS-1 to a cyclooxygenase active form. Mutants, in which three or four hydrophobic residues of the helices expected to protrude into the membrane, were replaced with small neutral residues. These mutants (often misfolded aggregates) exhibited little or no catalytic activity when expressed in COS-1 cells.

Interestingly, a similar mode of membrane anchoring via amphipathic helices has been recently suggested in the case of squalene cyclase (Wendt et al. 1997, 1999). PGHS and squalene cyclase share structurally similar

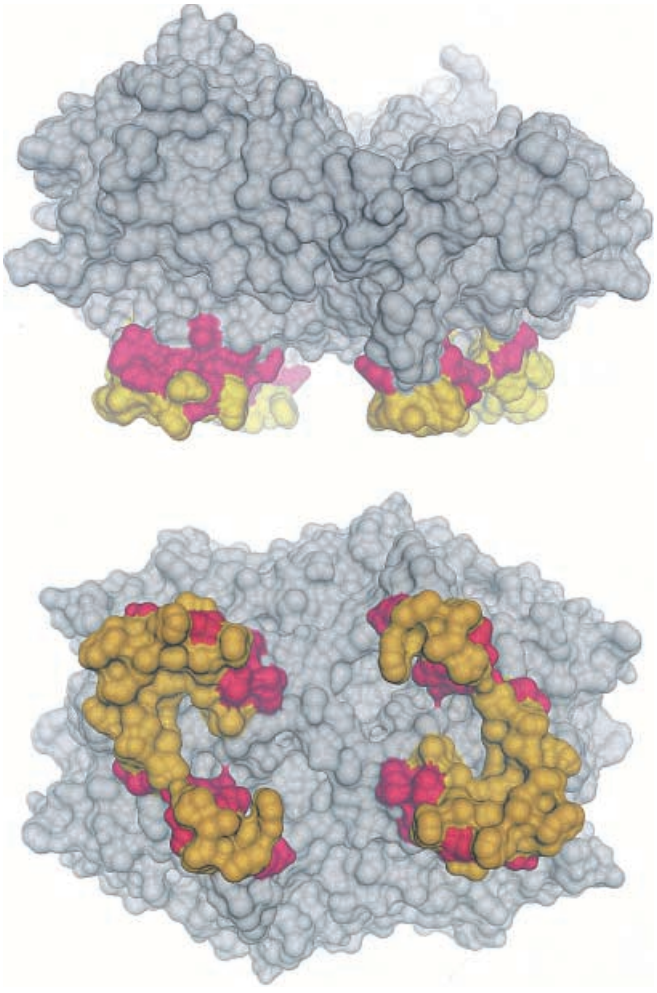

Fig. 2 DINO/MSMS (Philippsen 1999; Sanner et al. 1995) representation of the molecular surface of the PGHS-1 dimer. The hydrophobic residues surface is colored in yellow and the hydrophilic residues surface is red. Two viewing directions parallel and perpendicular to the molecular two-fold axis

membrane anchoring motifs but have little or no sequence similarity. The membrane anchoring region of the squalene cyclase forms a flat nonpolar plateau (consisting of one α-helix, one loop and one segment between two α-helices) and encircled by a ring of positive charged residues (Wendt et al. 1997, 1999).

According to the proposed model, PGHS-1 is a monotopic membrane protein since the binding motif does not extend beyond one leaflet of the bilayer. Thus, PGHS-1 and squalene cyclase are interesting from a structural point of view since they provide the first high-resolution structures of peripheral membrane proteins (Loll et al. 1995; Picot et al. 1994; Wendt et al. 1997). However, although the X-ray structure is suggestive, the detailed mode of interaction involved in the stable anchoring of PGHS cannot be elucidated based on the available experimental data. There is not enough information at the present time to completely determine the location and orientation of the membrane-bound form of the protein relative to the bilayer surface. A better understanding of the factors responsible for the interaction of PGHS-1 with a membrane would provide some insight into the attachment mechanism of peripheral membrane proteins in general. In addition, the proposed model has also some important functional implications for the cyclooxygenase activity of PGHS-1. The four-helices binding motif forms the entrance to a long narrow hydrophobic channel extending from the membrane surface and leading to the cyclooxygenase active site (Picot et al. 1994), which could be the pathway for the entry of arachidonic acid, the substrate of the cyclooxygenase activity. Unlike PGHS, such a polar pathway is not required for the function of squalene cyclase because its substrate (squalene) is entirely nonpolar (Wendt et al. 1997, 1999). Arachidonic acid is principally produced by phospholipidase A_2 (Smith et al. 1991). It is released into the hydrocarbon core of the lipid bilayer, where it is likely to remain because of its hydrophobicity. However, its movement from the membrane to the active site lying at the top of the hydrophobic channel has not been elucidated. A possible mechanism is that arachidonic acid penetrates directly into the cyclooxygenase active site from the interior of the bilayer through helices A, B and C of the anchoring domain without going into the bulk solvent region. The positively charged arginines of the anchoring domain may contribute to facilitate the movement of arachidonic acid in the channel leading to the cyclooxygenase active site through an interaction of the Arg120 guanidinium group with the arachidonate carboxylate group. It has been suggested that the carbonyl group of arachidonic acid interacts with Arg120 and Tyr385 and may determine the stereoselectivity of PGHS-1 for inhibitors (Bhattacharyya et al. 1996). Mutagenesis studies confirmed that the Arg120 residue of PGHS-1 is critical for binding the substrate and inhibitors through ionic interactions of its guanidinium group with the carboxylate moieties of arachidonic acid and some NSAIDs (Bhattacharyya et al. 1996; Mancini et al. 1995; Rieke et al. 1999). In view of its structural as well as functional implications, it is important to better characterize the membrane attachment of PGHS-1.

The goal of this paper is to examine the microscopic basis of the model proposed by Picot et al. (1994) for the anchoring of PGHS-1 to a membrane using computational methods. Two complementary approaches were used. First, the optimal configuration of the anchoring domain relative to the membrane was examined with implicit continuum models used to describe the protein solvation free energy. Second, two detailed atomic models of the anchoring domain bound to a solvated dimyristoylphosphatidylcholine (DMPC) bilayer were constructed and simulated with molecular dynamics (MD). The theoretical methods employed are described in the next section. Then the results are described and discussed. The paper is concluded with a brief summary of the main results.

Theory and methods

Mean-field continuum solvation model

Solvation effects provide the major force driving the association of proteins to membranes (Ben-Tal et al. 1996; Bernèche et al. 1998; Edholm and Jahnig 1988; Eisenberg and McLachlan 1986; Milik and Skolnick 1993). To investigate the importance of various energetic factors in the membrane association of the anchoring domain of PGHS-1, a mean-field potential based on a continuum approximation was used. A similar approach has been used previous by BenTal et al. (1996) and Bernèche et al. (1998). The total free energy of solvation ΔG_{tot} is decomposed into a nonpolar cavity formation ΔG_{np} and an electrostatic contribution ΔG_{elec} (Boresch et al. 1994; Gilson and Honig 1988):

$$\Delta G_{\text{tot}} = \Delta G_{\text{np}} + \Delta G_{\text{elec}} \tag{1}$$

The term ΔG_{np} accounts for the nonpolar contributions and is assumed to be related to the water accessible surface area of the protein. Assuming that the membrane normal is oriented along the Z-axis, a simple sum over the water accessible surface area of all atoms is used to approximate the nonpolar contribution:

$$\Delta G_{\text{np}}(Z) = -\sum_i S_i^{\text{np}} \gamma f(z_i) \tag{2}$$

where z_i is the position of the ith atom along the Z-axis, S_i^{np} is the water accessible surface area of the ith atom, and $\gamma = 33$ cal mol^{-1} Å^{-2} is the surface tension coefficient obtained from experimental free energies of the transfer of hydrocarbons from the pure liquid alkane to water (Hermann 1972). The function $f(z)$ models the transition from pure water to pure alkane at the interface:

$$f(z) = \begin{cases} e^{-(|z|-Z_0)^2/\Delta Z^2} & \text{if } |z| \geq Z_0 \\ 1 & \text{otherwise} \end{cases} \tag{3}$$

where Z_0 and ΔZ are the width of the core region and the width of the core region-polar heads interface, taken to be 10.0 and 2.5 Å, respectively, according to experimental data on lipid bilayers (Jacobs and White 1989; White and Wiener 1996). The water accessible surface area S_i^{np} was calculated by rolling a 1.4 Å probe on the protein van der Waals surface while atomic radii were taken from the all-hydrogen PARM22 force field (Mackerell et al. 1998).

The term ΔG_{elec} accounts for the reaction field contribution to the free energy of the peptide in the nonuniform dielectric media. The electrostatic contribution to the free energy of transfer from water to the membrane along the Z-axis was computed using the Poisson equation for macroscopic continuum electrostatics (Honig and Nicholls 1995; Honig et al. 1993; Warwicker and Watson 1982):

$$\nabla[\epsilon(\boldsymbol{r})\nabla\phi(\boldsymbol{r})] = -4\pi\rho^{\text{prot}}(\boldsymbol{r}) \tag{4}$$

where $\epsilon(\boldsymbol{r})$ is the position-dependent dielectric constant and $\rho^{\text{prot}}(\boldsymbol{r})$ is the charge density due to the protein. The protein was represented at the microscopic level with its associated atomic radii and atomic charges. All individual helices and the anchoring domain were treated as neutral. Specifically, blocking groups preserving the adjacent atoms of the amide plane were used to preserve the neutrality of the helical segments (CH_3-CO- for N-terminus and -NH-CH_3 for C-terminus). The atomic charges were taken from the all-hydrogen PARM22 force field (Mackerell et al. 1998); the atomic radii used to define the protein-solvent dielectric interface were derived from radial solvent charge distribution functions of the explicit solvent around the 20 standard amino acids (Nina et al. 1997). It was shown previously that this approach is able to yield a quantitative representation of the electrostatic contribution to the solvation free energies of amino acids that is consistent with thermodynamics perturbation techniques and MD simulations with an explicit model of the solvent (Nina et al. 1997). In the continuum electrostatic calculations, the membrane was represented by a planar slab of 25 Å thick corresponding to the width of the hydrocarbon core of the membrane (White and Wiener 1996). Dielectric constants were assigned according to the polarity of the medium: $\epsilon = 80$ for bulk water, $\epsilon = 2$ for the membrane and $\epsilon = 1$ for the protein. Because of the uncertainty on the continuum description, no intermediate dielectric region was assigned to the water-lipid interface and the region corresponding to the polar headgroups was assumed to have a dielectric constant of 80.

All calculations were performed with a cubic grid of 80 Å with two grid points per Å. The membrane geometrical center was translated to −15 Å along the Z-axis of a three-dimensional cubic grid. The ionic strength of the surrounding bulk solution was set to zero (no counterions were included). The protein was mapped onto the grid with its backbone center of mass placed at a distance Z from the geometrical center of the membrane. For each value of Z, the electrostatic contribution to the free energy of transfer from the water to the membrane was calculated by subtracting the electrostatic energy computed in a continuous medium representative of water from the electrostatic energy computed in a membrane immersed in a solvent region:

$$\Delta G_{\text{elec}} = \frac{1}{2}\sum_i q_i\left[\phi^{\text{memb}}(\boldsymbol{r}_i) - \phi^{\text{bulk}}(\boldsymbol{r}_i)\right] \tag{5}$$

where q_i is the charge of the ith atom in the protein, $\phi^{\text{memb}}(\boldsymbol{r}_i)$ is the total electrostatic potential of the protein near the membrane, $\phi^{\text{bulk}}(\boldsymbol{r}_i)$ is the total electrostatic potential of the protein immersed in the bulk region [$\phi(\boldsymbol{r})$ is the solution of the Poisson equation]. Calculations were performed using the finite-difference algorithm of Klapper et al. (1986), as implemented in the PBEQ facility (Beglov D, Im W, Roux B, unpublished) of the biomolecular simulation program CHARMM (Brooks et al. 1983).

Construction of the microscopic models

The membrane-bound three-dimensional conformation of the PGHS-1 anchoring domain was modeled using the 3.5 Å resolution X-ray structure available from the Protein Data Bank (Picot et al. 1994), and modified as described in the section Results and discussion. Only a single monomer was considered in the current computations to limit the number of atoms. Blocking groups preserving the adjacent atoms of the amide plane were used for the N-terminus (CH_3-CO-) and the C-terminus (-NH-CH_3). The atomic model used for the MD simulations is composed of the 54 amino acids anchoring domain of one PGHS-1 monomer (helices A, B, C and D), 71 DMPC molecules and 2938 water molecules, for a total of 18,129 atoms. This constitutes the central unit of a periodic system, the dimensions of which are 48×56 Å^2 in the xy directions. The membrane normal was oriented along the Z-axis. The two-fold crystallographic dimer axis (Picot et al. 1994) was assumed to be parallel to the bilayer normal and the corresponding orientation of the monomeric anchoring domain was preserved.

There are 29 and 42 lipids in the upper and lower halves of the bilayer, respectively. The four helix motif was anchored in the upper part of the membrane. Periodic boundary conditions were applied in the xy directions to mimic an infinite planar bilayer. A translation distance corresponding to the elementary box size along the Z-axis was used along the Z-axis to simulate a periodic multilayer system. The potential energy function used for the calculations was the all-hydrogen PARM22 force field (Mackerell et al. 1998) of the biomolecular CHARMM program (Brooks et al. 1983) which includes lipid molecules (Schlenkrich et al. 1996). The TIP3P model was used to represent the water molecules (Jorgensen et al. 1983). The hydrogen positions of the protein were constructed using the CHARMM subroutine HBUILD (Brunger and Karplus 1988). Adopted Newton-Raphson basis and steepest descent algorithms were used for the energy minimizations (Brooks et al. 1983).

A careful construction of such complex system is required in order to obtain a starting configuration that is representative of the solvated protein-membrane system. The general protocol developed by Woolf and Roux (1994, 1996) was used to construct the initial model. Such method has been used previously to generate other protein-membrane systems such as the gramicidin channel (Woolf and Roux 1994, 1996), bacteriophage Pf1 (Roux and Woolf 1996) and melittin in lipid bilayers (Bernèche et al. 1998). Since the

membrane-associated PGHS-1 anchoring domain is lying parallel to the surface of the bilayer, it is necessary to account for the cross-sectional area of the protein to determine the appropriate number of DMPC molecules to include in the upper and lower parts of the bilayer. The total cross-sectional area of the anchoring domain with its center of mass disposed at $Z = 0$ was determined as a function of Z. The cross-sectional area of the anchoring domain (not shown) varies from 100 $Å^2$ to a maximum of 780 $Å^2$ along the bilayer normal. The maximum in the cross-sectional area corresponds to the three amphipathic helices (A, B and C) lying parallel to the membrane plane and forming part of the membrane anchoring domain. The larger cross-sectional area of the protein corresponds roughly to that of 13 DMPC molecules. Assuming that the anchoring domain is bound to the upper halve of the bilayer, the simulation systems were constructed with 29 and 42 DMPC molecules in the upper and the lower halves of the bilayer, respectively, to accommodate the cross-sectional area of the PGHS-1 anchoring domain. To determine the initial position of each lipid relative to the protein, the effective lipid particles were modeled as a large Lennard-Jones sphere with a cross-sectional area of 64 $Å^2$, corresponding to the average cross-sectional area of one DMPC molecule in the liquid-crystalline L_α phase (Gennis 1989; Nagle 1993). Their packing around the protein was determined from a MD simulation in which the particles in both halves were restrained along $Z = \pm 17$ Å. The resulting spheres configurations were then replaced by full pre-equilibrated and pre-hydrated DMPC molecules chosen randomly from a library of 2000 DMPC molecules (Loof et al. 1991; Pastor et al. 1991; Venable et al. 1993). In this library, each phospholipid polar headgroup is pre-hydrated with approximately 20 water molecules. The number of bad contacts and atomic overlaps were reduced by performing systematic rigid-body rotations of the lipids around the Z-axis and translations in the xy-plane. One DMPC molecule of the upper half was manually disposed in the channel entrance formed by helices A, B, C and D. The total cross-sectional area of the entire DMPC/PGHS-1 system is 2690 $Å^2$. Finally, the system was fully hydrated by overlaying a pre-equilibrated box of water molecules of the appropriate dimension to obtain about 35 water molecules per lipid.

Two protein-membrane systems (I and II) were constructed with different membrane thickness. In system I, the thickness of the bilayer was kept identical to that of a pure lipid membrane. The dimension of the central unit of the periodic system is 48 Å × 56 Å × 68.4 Å and the center of the bilayer is at $Z = 0$. In system II, the membrane thickness was reduced to account for the presence of the anchoring domain. Because of the presence of the anchoring domain, there is a large vacuum created in the upper half of the bilayer with the current construction protocol. Such a large defect is unrealistic. In a fully relaxed and equilibrated system the thickness of the upper layer may be expected to be significantly perturbed by the presence of the protein. To deduce the thickness of the upper layer, we assume that the density from the carbon acyl chains is roughly similar in both the upper and lower halves of the bilayer. The density is n/V, where n is the number of DMPC molecules and V is the volume of the lipid core region of a layer. The volume of a layer is equal to the area of the bilayer times the thickness of the core region for that layer. The thickness of the lower layer, constituted of 42 lipids and no protein, was set to 12 Å in accord with scattering data (White and Wiener 1996). The density of the layer is $42/12 = 3.5$ lipids $Å^{-1}$.

Thus, the thickness of the upper layer constituted of 29 lipids should be equal to $29/3.5 = 8.3$ Å. To yield a similar density in both layers the bilayer of system II was assembled with the upper headgroups of the upper and lower halves located at $Z = -13.3$ Å and $+17$ Å, respectively. The dimension of the central unit of the periodic system II is 48 Å × 56 Å × 64.7 Å and the center of the bilayer is at $Z = +1.85$ Å.

Equilibration and simulation procedures

Two atomic systems of PGHS-1 anchored to a bilayer differing in the thickness of the membrane were equilibrated and simulated (systems I and II). The trajectories were calculated in the microcanonical ensemble with a constant number of atoms, volume and energy (NVE). The average temperature of the system was set to 330 K, above the gel-liquid phase transition of DMPC (Gennis 1989). The list of nonbonded interactions was truncated at 12 Å using a group-based cutoff. The electrostatic and van der Waals interactions were smoothly switched to zero from 8–11 Å. Since our main interest is to examine the structural reorganization in the hydrocarbon core of the membrane which rapidly takes place in response to the presence of the anchoring domain, we do not expect that the truncation of the nonbonded interactions has an impact on the current observations. The equations of motion were integrated with a time-step of 2 fs. The length of all bonds involving hydrogen atoms was fixed with the SHAKE algorithm (Ryckaert et al. 1977). The center of mass of the protein was kept at the center of the membrane plane in the xy-plane.

In the initial stage, the protein was fixed in place to prevent large spurious motions. In addition, various energy restraints were used to ensure a smooth transition of the atomic systems toward a relaxed configuration. Planar harmonic restraints were applied to the center of mass of the lipid polar headgroups (at $Z = \pm 17$ Å for system I and $Z = -13.3$ Å and $+17$ Å for system II) to maintain the planarity of the membrane. Planar repulsive potentials were used to prevent excessive penetration of water molecules into the hydrocarbon region (within $|Z| < 10$ Å). The two systems were optimized and relaxed with molecular dynamics simulation for 115 ps. Following this initial stage, the configurations of the two systems were further relaxed in the presence of harmonic restraints of 0.5 kcal mol^{-1} $Å^{-1}$ applied to the non-hydrogen atoms of the backbone of the anchoring domain. No restraints were applied to the protein side chains. This second stage of equilibration lasted 150 ps for system I and 100 ps for system II. The restraints on the lipids were gradually reduced to zero during the entire equilibration.

Following the equilibration, two types of trajectory were generated for systems I and II starting from their configurations at the end of the equilibration period: restrained (r) and unrestrained (u). First, trajectories of systems I and II were generated for 400 ps in the presence of harmonic restraints of 0.5 kcal mol^{-1} $Å^{-1}$ applied to the nonhydrogen atoms of the backbone of the protein to study the reorganization of the membrane structure around the anchoring domain in its native conformation (trajectories I/r and II/r). Second, trajectories of the two systems with no restraints applied to the protein were generated to examine the stability of the isolated anchoring domain (trajectories I/u and II/u). An unrestrained trajectory of 1 ns was generated for system I. The corresponding unrestrained trajectory was interrupted after only 200 ps in the case of system II because the anchoring domain exhibited significant structural distortions.

Results and discussion

Free energy of the anchoring domain and individual helices

The solvation free energies of the complete anchoring domain and the individual helices A, B, C and D were calculated along the Z-axis with a continuum representation of the environment as described in Theory and methods. The two-fold crystallographic dimer axis (Picot et al. 1994) was assumed to be parallel to the bilayer normal and all the molecular fragments (anchoring domain or individual helices A, B, C and D) were kept in their corresponding orientation. The results for helices A, B and C are shown in Fig. 3a–e. The optimal positions along the Z-axis according to the binding free

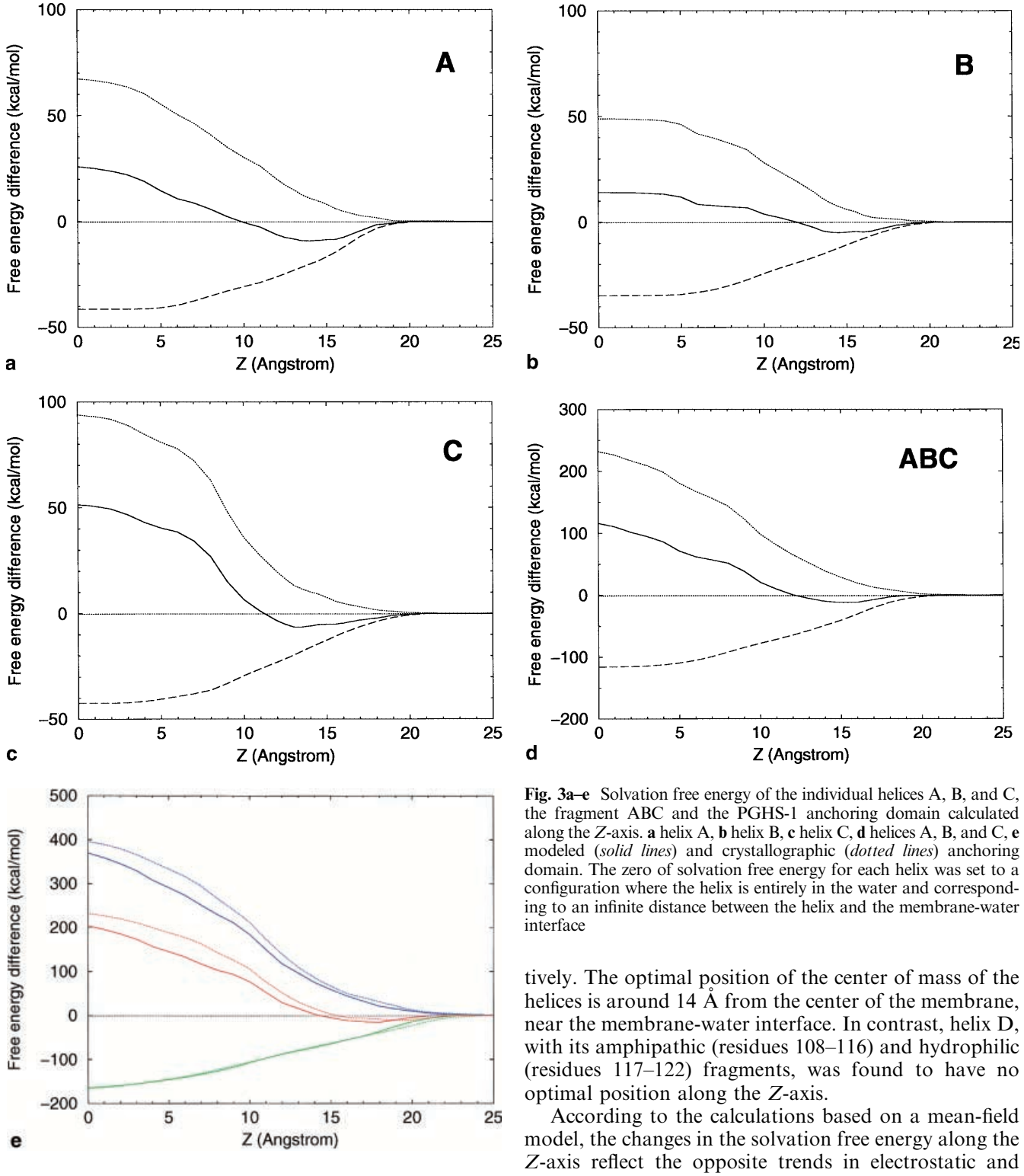

Fig. 3a–e Solvation free energy of the individual helices A, B, and C, the fragment ABC and the PGHS-1 anchoring domain calculated along the *Z*-axis. **a** helix A, **b** helix B, **c** helix C, **d** helices A, B, and C, **e** modeled (*solid lines*) and crystallographic (*dotted lines*) anchoring domain. The zero of solvation free energy for each helix was set to a configuration where the helix is entirely in the water and corresponding to an infinite distance between the helix and the membrane-water interface

energies are reported in Table 1. A result of significant interest is the existence of a free energy minimum for the individual helices A, B and C, near the lipid-water interface, at which point each helix is partially inserted into the bilayer in accord with their amphipathic character. In their optimal positions helices A, B and C are stabilized by −9.3, −5.1 and −6.5 kcal mol^{-1}, respectively. The optimal position of the center of mass of the helices is around 14 Å from the center of the membrane, near the membrane-water interface. In contrast, helix D, with its amphipathic (residues 108–116) and hydrophilic (residues 117–122) fragments, was found to have no optimal position along the *Z*-axis.

According to the calculations based on a mean-field model, the changes in the solvation free energy along the *Z*-axis reflect the opposite trends in electrostatic and cavity contributions. When the hydrophobic residues in the membrane side of the helices begin to interact with the membrane-water interface, the electrostatic contribution increases while the nonpolar contribution decreases. Helices A, B and C are stabilized near the membrane-water interface where the hydrophobic contribution is predominant compared to the electrostatic term. The electrostatic contribution becomes increas-

Table 1 Optimal positions along the Z-axis normal to the membrane plane according to the binding free energies (in kcal mol^{-1}) for helices A, B and C, the fragment (ABC) and the complete anchoring domain (ABCD). Z is the center of mass distance from the center of the membrane (in Å)

	X-ray				Modeled			
	Individual helices		ABCD		ABCD		ABC	
	Z	ΔG_{solv}	Z	ΔG_{solv}	Z	ΔG_{solv}	Z	ΔG_{solv}
A	14.0	−9.3	15.5	–	15.7	–	14.4	–
B	14.5	−5.1	21.6	–	16.9	–	15.6	–
C	13.0	−6.5	16.8	–	15.4	–	14.2	–
ABC	–	–	18.1	–	16.3	–	15.0	−12.1
ABCD	–	–	19.5	−11.0	18.0	−15.1	–	–

ingly unfavorable as the helix is inserted into the membrane, reflecting the energetic cost of transferring the polar backbone from the aqueous phase to the nonpolar membrane region. At $Z = 0$ Å the helix is completely inserted into the membrane and the solvation free energy is largely dominated by the unfavorable electrostatic contribution. A single minimum is observed in $\Delta G_{tot}(Z)$. No free energy barrier opposing the association of the individual helices or the anchoring domain is observed. A similar trend has been observed previously in continuum electrostatic calculations by Ben-Tal et al. (1996) for the association of a simple polyalanine helix with a membrane and by Bernèche et al. (1998) for the association of melittin with a membrane. In the optimal configuration, the center of mass of the anchoring domain is at $Z = 19.5$ Å and the free energy of association is −11.0 kcal/mol (Fig. 3e). In this position, the center of mass of helices A, B and C are at $Z = 15.5$, 21.6 and 16.8 Å, respectively, as indicated in Table 1. The hydrophobic face of each helix interacts with the low dielectric region whereas the hydrophilic residues are in the high dielectric region. Since the lipid-water interface is located at 12–14 Å the individual helices are not in their respective optimal positions when the entire anchoring domain is translated as a whole. Helices A and C are partially inserted into the core membrane slab whereas helix B is out of the membrane in the optimal position, as shown in the top of Fig. 4.

Structural modification of the anchoring domain

Even though each individual amphipathic helix exhibits a well-defined free energy minimum in Fig. 3, the crystallographic structure of the anchoring domain does not appear to be consistent with the binding of amphipathic surface-active peptides at a membrane-water interface (Eisenberg et al. 1982; Kaiser and Kezdy 1987). In particular, helix B is 6 Å above helices A and C along the dimer two-fold symmetry axis (Picot et al. 1994). Results by Spencer-1999 based on the analysis of site directed mutants indicate that the amphipathic character of each helix (A, B and C) is important for the assembly and folding of PGHS-1, suggesting that they each bind to a membrane surface environment. A plausible mode of association of PGHS-1 with a membrane would thus require that all three amphipathic helices are located at the membrane-water interface. However, according to the mean-field free energy model, helices A, B and C are not at their respective optimal positions (see Table 1) when the whole anchoring domain is at the membrane surface. These observations suggest that the relative position of the helices in the anchoring domain in the membrane-associated form might differ slightly relative to the crystallographic structure. Some structural variation of the membrane anchoring domain in the crystal

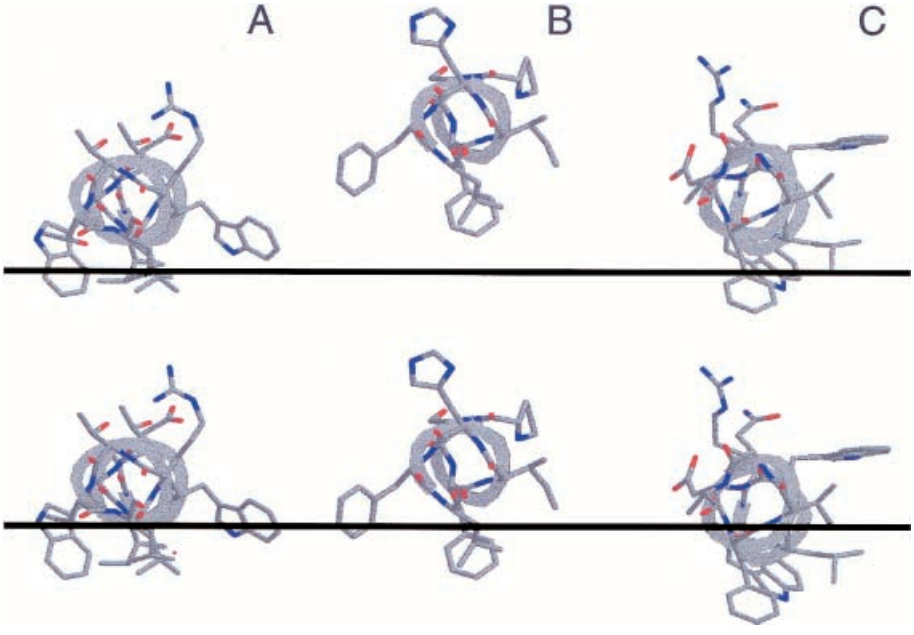

Fig. 4 Wheel representation of the interfacial position of the helices forming the anchoring domain in the crystallographic (*top*) and modeled structure (*bottom*) showing that helix B is notably higher than helices A and C with respect to a plane defined at $Z = 12.5$ Å from the center of the bilayer as used in the continuum model for protein-membrane association

are possible because of the detergent environment (Picot D, Garavito RM, personal communication). For example, small structural differences in the four-helices binding motif have been reported between PGHS-1 and PGHS-2 (Luong et al. 1996). More generally, some structural variability in the hydrophobic region of membrane proteins is not uncommon. In particular, structural differences have also been observed in two crystal forms of *Escherichia coli* Ompf porins (Cowan et al. 1992, 1995).

To account for an adaptation of the anchoring domain to the membrane-water interface, the experimental structure of the PGHS-1 binding motif was modified according to the optimal free energy positions obtained for the three individual helices. All changes concern only the translation of the center of mass along the Z-axis. Each helix was translated to its global free energy minimum position. Since it does not possess a minimum, helix D was translated together with helix C to its optimal position. After translation of the helices, the modified anchoring domain was relaxed using energy minimizations on the loops internal coordinates while the four helices were kept fixed. The modified configuration is more stable than the crystallographic structure by 6.6 kcal mol^{-1} after energy minimization in vacuum. The structural changes involved only the loops A-B, B-C and C-D, and the relative center of mass position of helices A, B and C. The geometry of the side chains was unchanged. The interfacial position of the helices A, B and C before and after the modification of the anchoring domain is illustrated in Fig. 4.

The resulting structure of the anchoring domain superimposed to the crystallographic structure (Picot et al. 1994) is shown in Fig. 5. The structural changes are modest. The root-mean-squared (RMS) coordinate difference of the anchoring domain before and after the modification is 2.3 Å for the nonhydrogen atoms of the loops (1.6 Å for the backbone atoms of the loops).

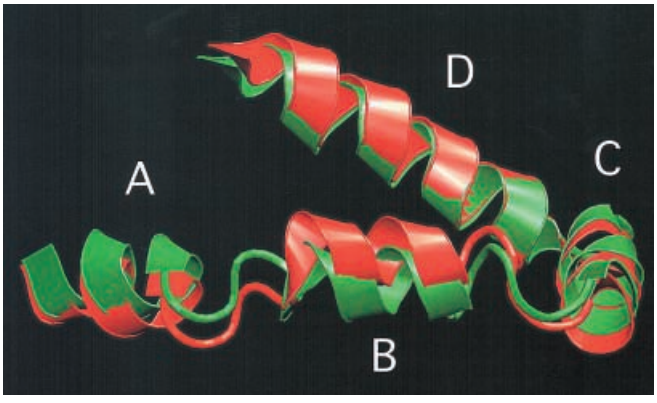

Fig. 5 The binding motif of PGHS-1 is formed by three amphipathic helices A, B, C and the beginning of helix D in the X-ray structure of Picot et al. (1994) (*in red*). The modified anchoring domain (*in green*) was obtained by translation of helices A, B and C to their minimum solvation free energy along the Z-axis perpendicular to the membrane plane

As shown in Fig. 5, helix B is closer to the positions of helices A and C in the modified anchoring domain than in the crystallographic structure and the three helices (A, B and C) form a planar motif. The modified anchoring domain is in better accord with the concept of association of amphipathic helices at a membrane-water interface than the crystallographic structure (Eisenberg et al. 1982; Jacobs and White 1989). As shown in Table 1, helices A and C are translated towards the lipid-water interface by 1.5 and 3.8 Å, respectively. Notably, after translation by 7.1 Å towards the low dielectric region, helix B is closer to the membrane-water interface as shown in the bottom of Fig. 4.

The association free energy of the modeled anchoring domain estimated with the continuum mean-field potential is plotted in Fig. 3e. The result suggests that the binding motif is stabilized by about −15.1 kcal mol^{-1} when its center of mass is located at $Z = 18.0$ Å. In the optimal configuration the center of mass position of each helix is not exactly at the minimum found from the calculations performed on the individual helices because of a global translation of the anchoring domain towards the high dielectric medium by 2 Å (see Table 1). To elucidate this result, the potential ΔG_{tot} was calculated for the modified anchoring domain excluding helix D (i.e. for helices A, B and C alone). The results of the calculations for this ABC motif are shown in Fig. 3d and in Table 1. The ABC motif is stabilized by −12.1 kcal mol^{-1} when its center of mass is located at $Z = 15.0$ Å. Each helix is located at its optimal position within 1 Å, as shown in Table 1. The free energy of the anchoring domain formed by helices ABCD is −15.1 kcal mol^{-1} at $Z = 18$ Å, whereas the free energy of the anchoring domain formed by helices ABC is −12.1 kcal mol^{-1} at $Z = 15$ Å. The solvation free energy of the full anchoring domain is 3 kcal mol^{-1} more favorable than for the ABC motif. Thus, although the optimal position is shifted towards the bulk region, the presence of helix D contributes to stabilize the anchoring domain to the membrane. Decomposition of the mean-field free energy indicates that helix D provides further stabilization to the anchoring domain by decreasing the nonpolar contribution ΔG_{np}.

The total solvation energy of the ABC motif (−12.1 kcal mol^{-1}) is not equal to the sum of the solvation energies of the individual helices A, B and C (sum of the terms of the second column of Table 1: −20.9 kcal mol^{-1}). This indicates that there are environment-mediated interactions between the three helices within the anchoring domain.

Simulations with an explicit membrane

The implicit mean-field continuum model is based on a number of approximations and provides only a simplified view of the membrane environment. To examine the membrane association of PGHS-1 from a microscopic point of view, two atomic models consisting of the

anchoring domain of one PGHS-1 monomer bound to a fully hydrated DMPC membrane were constructed and simulated with molecular dynamics.

The structurally modified anchoring domain was used as the initial model for subsequent molecular dynamics simulations in an explicit environment. In the first model (system I) the PGHS-1 anchor domain was associated to a bilayer with a thickness identical to that of a pure bilayer. In the second model (system II) the membrane thickness was decreased to yield a similar carbon acyl chains density in both layers. Although previous studies show that very slow relaxation time scales are present in membranes (Pastor and Feller 1996), the length scale of the present simulations is sufficient to allow for the dominant structural reorganization and packing of the lipid hydrocarbon chains around the anchoring domain.

Average structure of membrane-protein systems

Figure 6 shows the structural changes occurring in the membrane structure during the equilibration period of systems I/r and II/r. The initial bilayer configurations of systems I/r and II/r are completely planar as a result of the construction protocol. In the early stage of the equilibration period of both systems, the ideal planarity of the membrane is rapidly altered by displacements of the lipids along the membrane normal. A similar behavior was observed previously in the simulation of melittin in a DMPC membrane (Bernèche et al. 1998). In addition, the order of the lipid acyl chains is decreasing in the upper layer while it is more or less stable for those in the lower layer. Such reorganization is more significant in system II/r than in system I/r, as shown in Fig. 6 (see snapshots after 100 ps). For system I/r the acyl chains of both layers contribute to fill the initial empty space due to the presence of the protein. The acyl chains of the upper layer are partially curled and those in the lower layer appear to be slightly more extended at the end of the equilibration period relative to the initial configuration. For system II/r a similar but more pronounced reorganization is observed, with the acyl chains in the top layer being more disordered than in system I/r. Because of this structural re-organization, the thickness of the hydrophobic core of the membrane is reduced by approximately 2 Å from its initial thickness for both systems.

The average density profile of systems I and II are shown in Fig. 7 (the helix D was excluded from the protein average density for the sake of clarity). For both systems the results indicate that the anchoring domain is

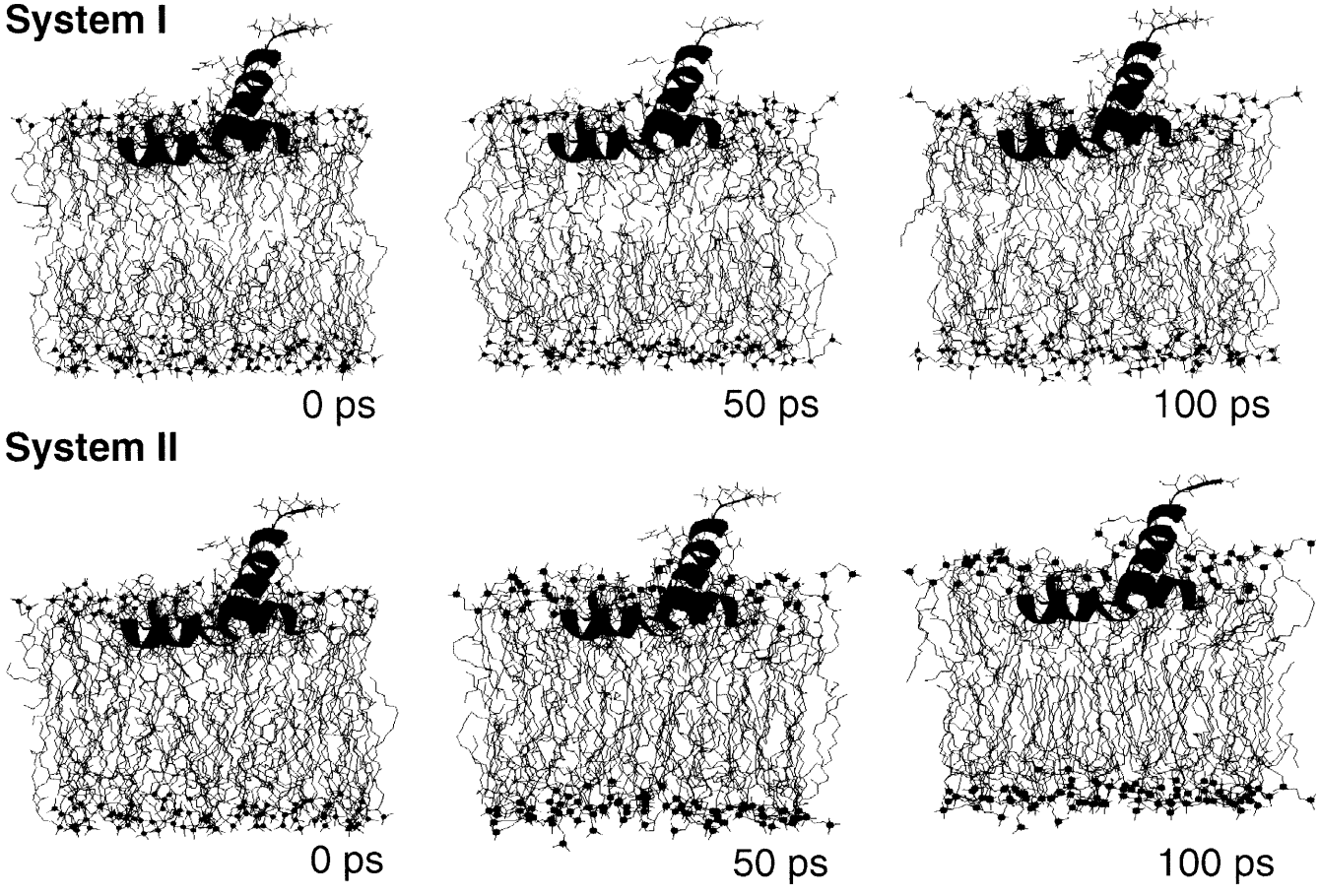

Fig. 6 Representation of the atomic system through the equilibration period of systems I/r and II/r. The deformation of the upper layer of the membrane is significant in both systems I and II

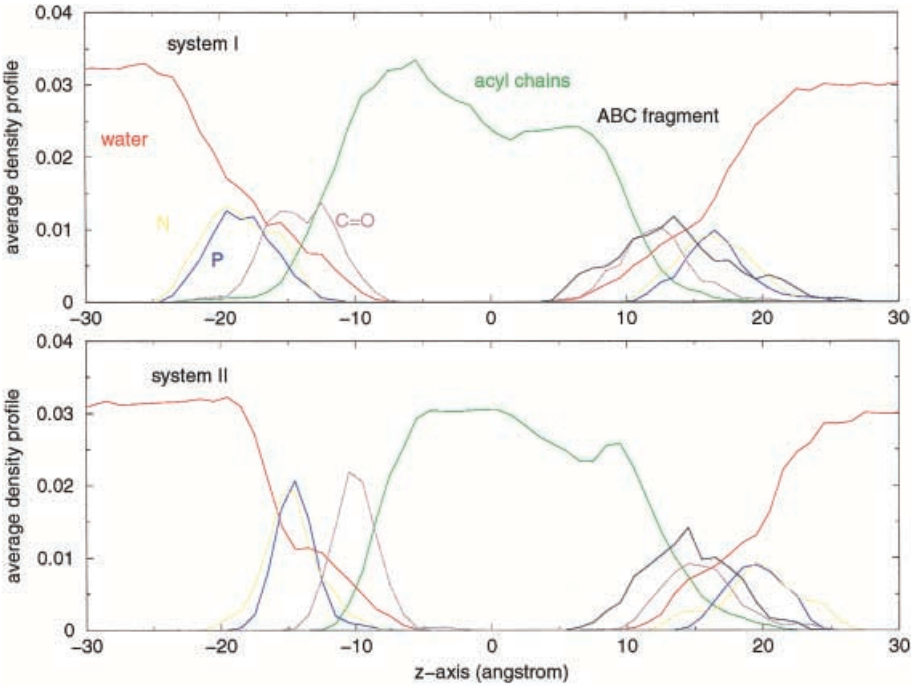

Fig. 7 Averaged density profiles of the protein, the lipids and water molecules along the Z-axis of systems I/r and II/r. The density profile of the heavy atoms of the PGHS-1 anchoring domain (helices ABC only), water and the hydrocarbon chains, the ester oxygens of the glycerol region, the headgroup phosphate and nitrogen of the DMPC lipid molecules are shown

associated only with the upper leaflet of the membrane. Such model for interaction, suggested by Picot et al. (1994), is characteristic of a monotopic membrane. The protein atoms go as deep as 5 Å from the center of the bilayer but the maximum density is at the membrane-water interface (about $Z = 15$ Å for both simulations). The thickness of the interfacial regions (defined by the density profile of the phosphate choline, and lipid carbonyl groups) of the top and lower layer depends on the system. For system I/r there is a local minimum in the density of the acyl chains density around $Z = 2.5$ Å. The average density profile of the acyl chains of system II/r is somewhat different, with a local minimum in the density of the acyl chains at about $Z = 8$ Å. The membrane-solution interface of the lower layer of system I/r is broader than that of system II/r, with 18 and 16 Å thickness, respectively. The thickness of the interface of the upper layer, which is associated with the anchoring domain, is the same for both systems (i.e. 20 Å). Such interfacial membrane broadening in the presence of a bound amphipathic protein has been observed in previous simulations (Bernèche et al. 1998). In both systems, the phosphate and choline in the lower and upper layer are located around similar positions along the membrane normal, reflecting the fact that the polar headgroups are oriented nearly parallel to the membrane-water interface. The main difference found between the two systems is the narrow density distribution of the choline, phosphate and C=O groups of the lower layer of system II/r compared to system I/r. This result indicates that the lower layer of the thinner membrane-protein system is more ordered.

The distribution of free volume in the systems provides useful information concerning the packing of the hydrocarbon chains in the membrane. The calculated free volume for the initial configuration, and averaged over the trajectories I/r and II/r, are shown in Fig. 8. Before any equilibration, both systems possess initially a large fraction of accessible free volume. The empty volume in the initial system is irregularly spread over the whole membrane region, with a maximum near $Z = +5$ Å. The large defect is, however, filled rapidly during the equilibration period. The comparison between the empty volume in the initial configuration and the equilibrated system shows a redistribution of the empty volume and a simultaneous decrease of the vaccum region under the amphipathic helices in systems I/r and II/r. As shown in Fig. 8, no empty space is left under the anchoring domain, as indicated by the distribution of the free volume in both systems I and II. The average density calculated over the trajectories I/r and II/r reveal a significantly smaller accessible free volume fraction (the maximum value is less than 0.05) compared to other results from protein-membrane simulations (Bernèche et al. 1998). Nonetheless, the largest density is at the center of the membrane, in accord with results obtained previously for pure membrane simulations (Marrink and Berendsen 1994) and an amphipatic helix bound at the surface of a membrane (Bernèche et al. 1998). This indicates that the phospholipid bilayer possesses a considerable ability to adapt (“plasticity”) to the large perturbation caused by the anchoring domain.

The structural plasticity of the membrane hydrocarbon core arises from the isomerization of the dihedrals angles of the acyl chains. The increased number of “kinks” in the lipid chains alters the packing in the hydrocarbon core of the bilayer. In the lower halve of the bilayer of trajectory of system I/r, large fluctuations were observed for most of the lipids, whereas the lower layer of trajectory II/r was found less mobile. The total

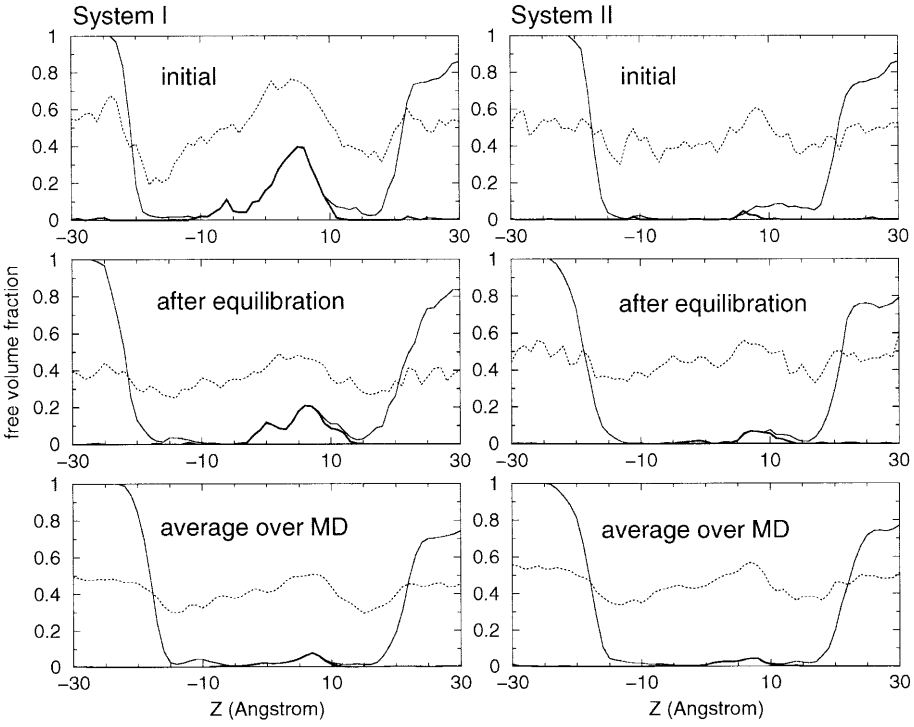

Fig. 8 Average empty volume (*dotted line*) and the accessible free volume to water molecules [excluding (*solid line*) and including (*bold line*) the water molecules of the system] present in the initial, equilibrated and averaged systems I/r and II/r

fraction of bonds in the *trans* state (defined by dihedral angles with a value around 180 ± 30°) is 67% for the upper layer and 71% for the lower layer in the case of system I/r. The corresponding fraction of *trans* is 38% for the upper layer and 71% for the lower layer in the case of system II/r. The fraction of *trans* for the lower layer is close to that of an unperturbed bilayer (Mendelsohn et al. 1989). Therefore, the upper layer appears to be most perturbed by the change in bilayer thickness, whereas the lower layer is relatively undisturbed.

Environment of the anchoring domain and functional implications

A more complete picture of the protein solvation is provided by characterizing the environment surrounding the side chains. The average number of nearest neighbors within a distance of 5 Å around each residue was calculated by integrating the individual radial distribution functions normalized by the total number of non-hydrogen atoms of the side chains. For systems I/r and II/r it was observed on average that the solvation of the helices forming the anchoring domain is in agreement with their amphipathic nature, as found in previous simulations of amphipathic helices at the membrane-water interface (Bernèche et al. 1998).

Figure 10a–d shows the average number of nearest neighbors for system I/r. Generally, the polar side chains are exposed to water whereas the nonpolar side chains are exposed to the lipid hydrocarbon chains. This is in qualitative accord with the experimental findings of Spencer et al. (1999). However, the average environment is more complex in the case of some nonpolar residues. For example, Ala105 side chain of helix C is exposed to water, choline, phosphate groups and hydrocarbon. A similar complex environment was found for Ala11 in the simulation of Pf1 coat protein in a phospholipid bilayer (Roux and Woolf 1996). The interaction of the four tryptophan residues (Trp75 and Trp77 of helix A, and Trp98 and Trp100 of helix C) with both the hydrocarbon chains and the water reflects the amphipathic character of the indole group. Such interactions contribute to stabilize the protein anchoring domain at the membrane-water interface, as discussed previously (Bernèche et al. 1998). Phe88 of helix B and Phe102 of helix C are completely buried in the core of the membrane whereas Phe107 of the connecting loop between helices C and D (not shown) is essentially solvated by the acyl chains. The four residues Phe contribute significantly to the binding of the protein to the membrane through hydrophobic interactions. It is observed that all charged side chains interact on average with the lipid polar headgroups and water with direct or indirect interactions. The four positively charged side chains of Arg residues (Arg79 of helix A, Arg83 of the connecting loop between helices A and B, Arg97 of helix C, Arg109 and Arg114 of helix D) are interacting on average with lipid headgroups as shown in the average density profile of Fig. 10a–d. The average number of nearest neighbors for system II/r was found very similar to the one of system I/r and is not shown here.

An instantaneous configuration of the system I/r during the dynamics simulation was analysed in terms of the microscopic interactions of the protein with its environment. The Glu73 carbonyl side chain of forms a hydrogen bond with a lipid phosphate group through a water molecule. The NH group of Trp75 forms a

hydrogen bond with a water molecule and the positively charged Arg79 side chain is completely solvated by water molecules. The selected instantaneous configuration of system I/r (not shown) reveals that two polar headgroups are interacting with each other above helix B. Trp98 interacts with a water molecule which penetrated into the membrane core. Near the helix's end, the carbonyl group of Ala105 interacts with a choline group. Interestingly, the side chain of Arg120 (helix D) was found directly hydrogen bonded to the phosphate group of a DMPC molecule in the channel entrance formed by helices A, B, C and D. Figure 9 shows the side chain of Arg120 interacting with the phosphate headgroup of a lipid molecule as found in the initial configuration and during the simulation of system I/r. The bound lipid occupies the region corresponding to the entrance of the hydrophobic channel leading to the active site of the full enzyme. The Arg120 residue is involved in the interaction with fatty acid substrates and inhibitors (Bhattacharyya et al. 1996; Rieke et al. 1999). In particular, this residue is necessary for the inhibition by NSAIDs of the cyclooxygenase active site containing a carboxylic acid moiety (Mancini et al. 1995). In all the current simulations (i.e. I/r, I/u, II/r and II/u) the lipid molecule inserted at the entrance of the channel diffused along the *Z*-axis to interact strongly with the guanidinium of Arg120. This suggests that a lipid molecule could occupy the hydrophobic channel when the arachidonic acid substrate is absent. Although further calculations with the full enzyme will be required to fully elucidate the mechanism of PGHS-1, these observations provide insights into the the association of the arachidonic acid substrate to the cyclooxygenase active site.

The atomic system of the membrane-bound anchoring domain can be used to construct a preliminary model of the entire PGHS-1, together with the EGF-like module and the catalytic domain. This is shown in Fig. 11. Interestingly, it is observed that the EGF-like module is located near the interface region and could, thus, contribute to stabilize the anchoring domain at the membrane-water interface.

Stability of the anchoring domain

To analyse the stability of the PGHS-1 anchoring domain at the membrane surface, a trajectory was generated for 1 ns with the protein unrestrained (I/u). The initial planarity and orientation of the four amphipathic helices are partially lost during the early stage of the unrestrained simulation, and the center of mass of the anchoring domain penetrates into the membrane by about 1 Å. Simultaneously, a rigid-body drift of each individual helix up to 3 Å relative to their initial position is observed after the release of all constraints on the protein. Each helix is undergoing motions with fluctuations on the order of 3–5 Å along the *Z*-axis. At the C-terminus, the end of helix D is surrounded by water and is fraying because of the absence of the rest of the enzyme. At the N-terminus, helix A remains stable along the trajectory. The average overall RMS deviations of the coordinates of all the nonhydrogen atoms relative to the initial and the crystallographic structures are 2.9 Å and 3.4 Å, respectively. The RMS deviations of the individual helices are significantly less then those for the overall anchoring domain, indicating that the structural changes are due to the rigid-body movements

Fig. 9a, b Interaction between Arg120 guanidinium side chain and the phosphate group of the inner lipid molecule based on the simulation of system I/r. **a** initial configuration and **b** during the trajectory. The lipid is stabilized in the entrance of the hydrophobic channel

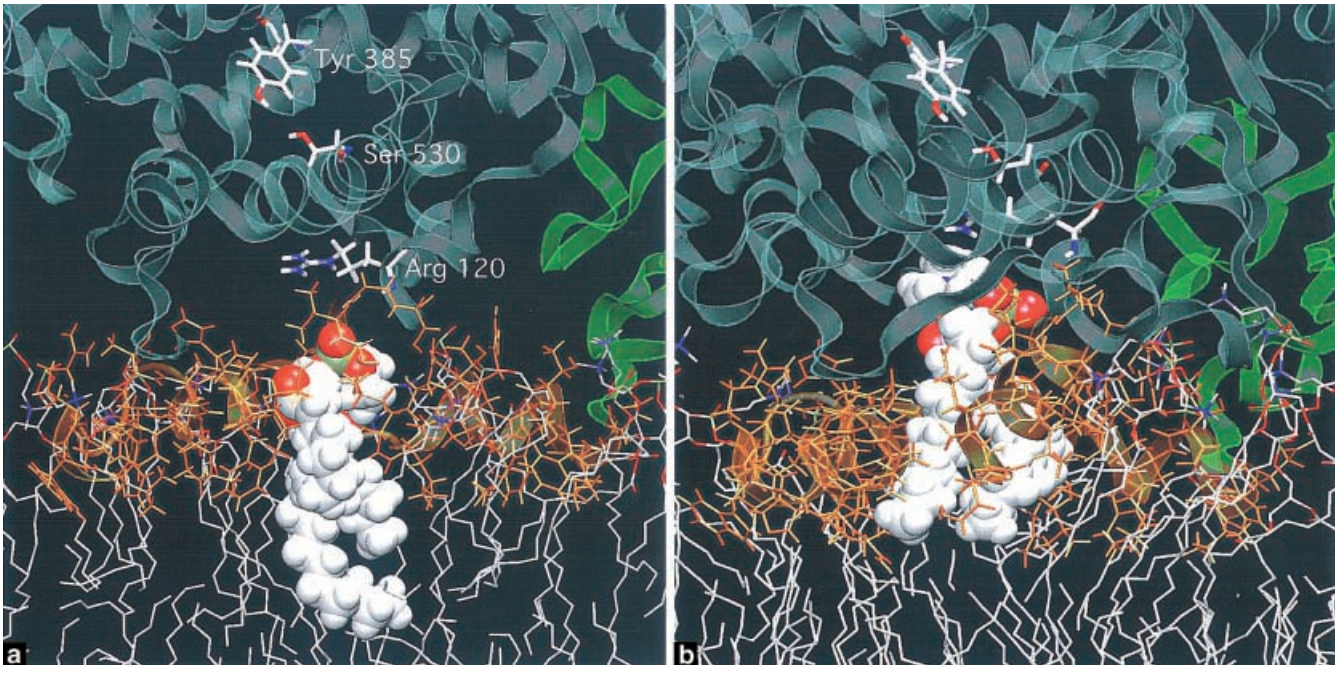

of the helices. The orientation of helix A relative to helix B remains close to its initial configuration for 600 ps, then decreases by about 20°. The angle formed by the helical axis of two consecutive helices fluctuates up to 20° around the experimental angle (i.e. A/B 143° and B/C 103°). The angle between the helices B and C remains at the vicinity of the crystallographic value for the first 300 ps, then decreases by 60°. Such significant changes occurring in the structure account for the RMS difference found previously. The results indicate that the fluctuations of the anchoring domain arise from the flexibility of the short inter-helical loops while the helices behave as relatively rigid units. A similar trajectory with the protein unrestrained was generated for system II (trajectory II/u). However, the simulation II/u was interrupted after 200 ps because the helices drifted towards the membrane core, yielding rapidly an unrealistic configuration in which helix C was solvated essentially by the lower layer acyl chains. The significant changes in the protein anchoring domain structure observed during the unrestrained simulations I/u and II/u might be indicative that the complete protein (i.e. the catalytic domain and the EGF-like module) is needed to stabilize the anchoring domain at a membrane surface. However, the lack of stability of the anchoring domain in the present simulations might also be due to the limitations of the computational models. Extensive simulations with different initial conditions would be necessary to explore the various factors contributing to the stability of the anchoring domain.

Fig. 10a–d Contribution from the main components of the system I/r to the solvation of the side chains of PGHS-1 anchoring domain. **a** helix A. **b** helix B. **c** helix C and **d** beginning of helix D

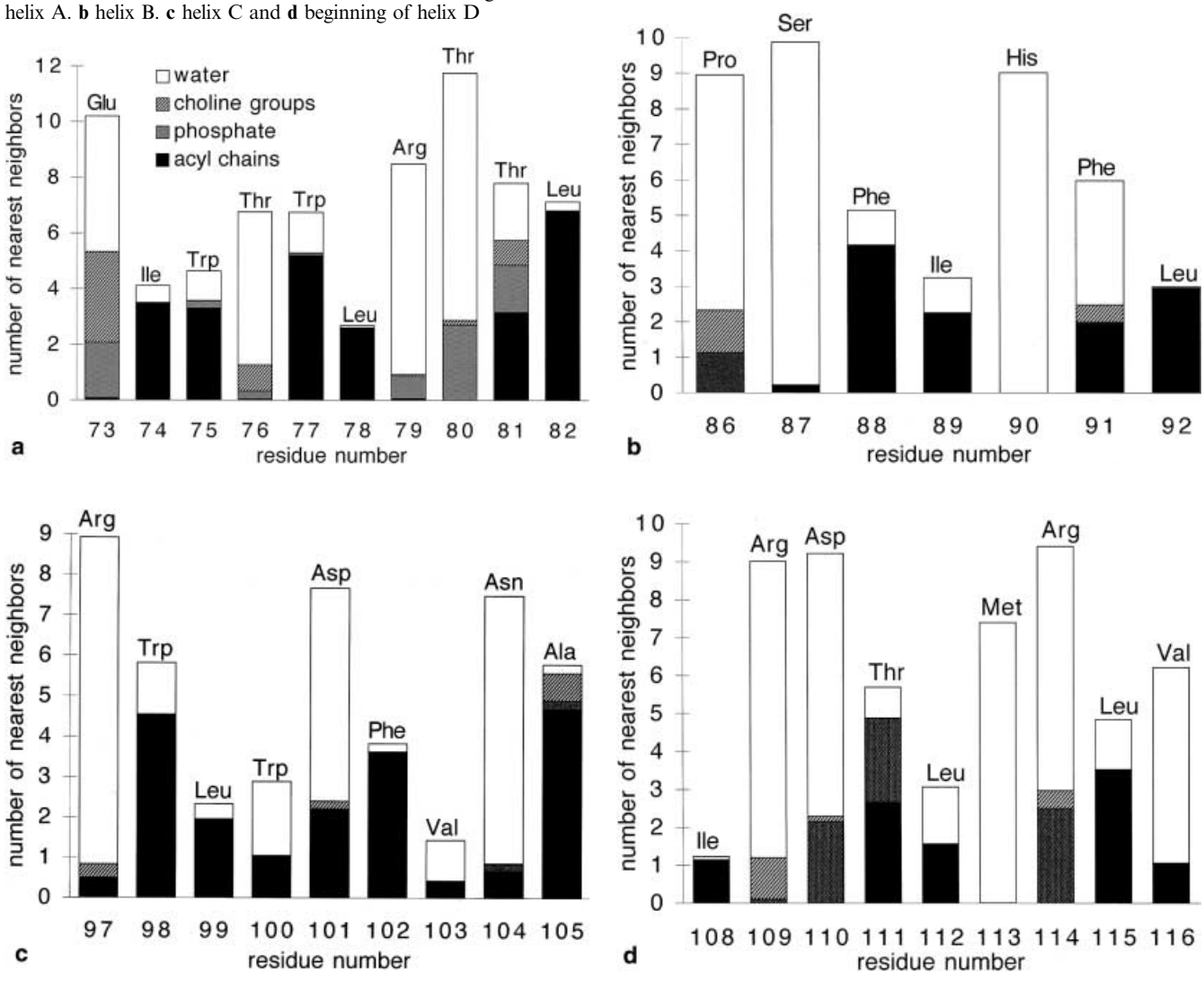

Summary

The membrane association of the anchoring domain of PGHS-1 was examined using complementary approaches. First, an implicit mean-field continuum model, in which the membrane was represented as a structureless slab of low dielectric material, was used to investigate the optimal configuration of the protein anchoring domain relative to the membrane. Because the

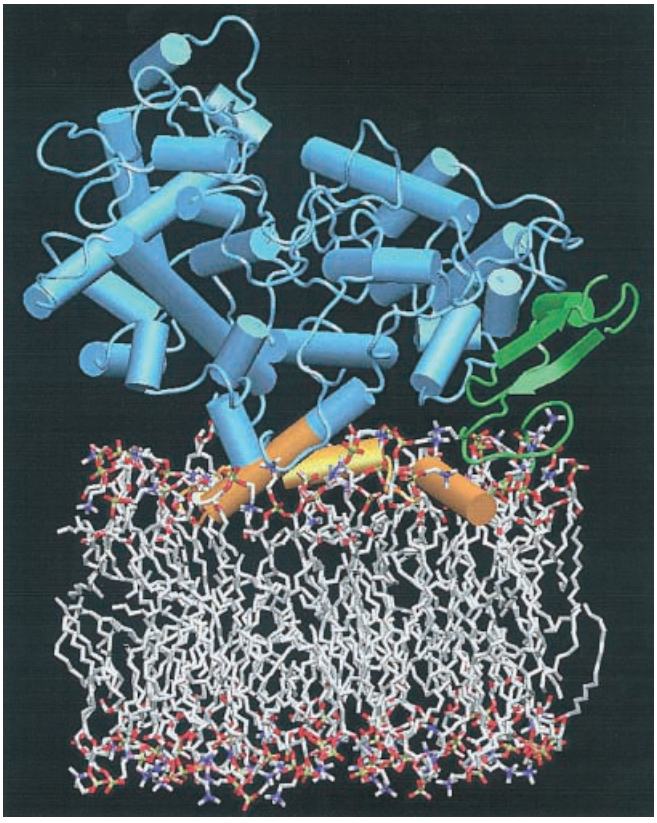

Fig. 11 Microscopic model of system I/r with one DMPC molecule placed by hand inside the cavity formed by helices A, B, C and D. The EGF-like module (*in green*) and the catalytic domain (*in yellow*) were added to the modelized binding motif (*in orange*)

continuum approach is computationally inexpensive, it can be advantageously used to explore the association of the anchoring domain with the interface over a range of depth. Second, molecular dynamics simulations of the anchoring domain with explicit membrane and solvent molecules were performed to provide a microscopic atomic model of the system. The purpose of those simulations was to examine the dominant structural reorganization required for the anchoring of a peripheral membrane protein such as PGHS-1. Clearly, the very slow relaxation time scales present in the bilayers suggest that several nanoseconds would be necessary for a complete sampling of all possible configurations (Pastor and Feller 1996).

The optimal positions of the anchoring domain as well as of each individual helix forming the anchoring domain were calculated and compared to their positions found in the optimal configuration of the complete anchoring domain. Free energy minima were found for the individual helices A, B and C, where each helix is located at the membrane-water interface; no optimal position was found for helix D. However, the individual amphipathic helices cannot be simultaneously located at an optimal position at the membrane surface if the anchoring domain is kept in the conformation in the crystallographic structure. This is in contrast to the observation that that the amphipathic character of each helix (A, B and C) is important for the assembly, folding and activity of PGHS-1 (Spencer et al. 1999). These considerations led us to the hypothesis that the anchoring domain of PGHS-1 deviates slightly from the X-ray structure upon binding to a membrane surface. The relative position of each helix was translated to its optimal position and helix D was translated together with helix C. The optimal position of the modified anchoring domain at the interface was better associated by about 4 kcal mol^{-1} with the membrane, providing a plausible initial configuration for the atomic model. The proposed structural modification of the anchoring domain of PGHS-1 relative to the X-ray structure could be tested experimentally. For example, it may be possible to use electron paramagnetic spectroscopy with site-directed spin-labeling techniques to detect the presence of structural variations in the anchoring domain and determine the exposure of the amphipatic helices to the aqueous and hydrocarbon phases (Perozo et al. 1999).

Atomic models with explicit lipids and solvent molecules were constructed for molecular dynamics simulations. In system I, the thickness of the bilayer was kept identical to that of a pure lipid membrane, whereas in system II it was reduced by 3.7 Å in order to fill the unrealistic vacuum created by the protein in the upper layer of the initial system and to maintain identical densities of lipid acyl chains in both layers. Simulations of the protein membrane systems without any restraints on the protein suggest that the entire catalytic domain and the epidermal growth factor-like module are required for the stability of the anchoring domain at the membrane-water interface, e.g. the helices (A, B and C) undergo rigid-body motions arising from the flexibility of the inter-helical loops. However, such fluctuations occur on a slow time scale and are incompletely averaged in the present simulation.

Simulations of the system with harmonic restraints on the protein (I/r and II/r) were used to analyse the structure of the lipids and their interactions with the anchoring domain. The observed exposure of the side chains of the amphipatic helices to water and hydrocarbon is in qualitative accord with the experimental results of Spencer et al. (1999). The average density profiles of the main components of sytems I/r and II/r show that the PGHS-1 binding motif interacts solely with the upper layer of the membrane. This result is in good accord with the definition of a monotopic protein. In both systems I and II the most important disorder of the lipid chains is observed in the upper layer. The hydrocarbon chains of the lipids are wrapped and curled around the helices lying parallel to the membrane plane. Such structural features appear to be required for the association of a protein possessing no transmembrane domain. Nonetheless, despite the large perturbation induced by the anchoring domain, the fraction of cavities in the hydrocarbon core of the bilayer is rapidly reduced at the beginning of the simulations. In the final configurations, the cavity fraction does not differ from that of

a pure lipid bilayer. The analysis of the membrane structure thus shows that the phospholipid bilayer possesses a remarkable plasticity and is able to adapt to the presence of a monotopic protein.

Interestingly, the present calculations suggest that a fatty acid molecule can be located at the center of the motif formed by helices A, B, C and D, which corresponds to the entrance to the long channel leading to the cyclooxygenase active site in the full enzyme. The DMPC molecule, which was manually inserted in the center of the ABCD motif, in the construction of the atomic systems, diffused from its initial position and formed a stable interaction with the guanidinium group of Arg120 in helix D. Further calculations with the full enzyme will be required to fully elucidate the movement of the arachidonic acid substrate into the cyclooxygenase active site.

The present work illustrates how two different approaches may be used in a complementary fashion to provide a sound basis for viewing protein-lipid interactions. However, although a critical examination of the atomic model in view of experimental data would be highly desirable, the absence of structural information about the membrane association of PGHS-1 does not permit such a comparison at this point. Future work will consider the configuration of a complete model of PGHS-1 anchored to a membrane.

Acknowledgements Numerous discussions with Michael Garavito and Daniel Picot are gratefully acknowledged. This work was supported by a grant from the Medical Research Council (MRC) of Canada. B.R. is a research fellow of the MRC.

References

Ben-Tal N, Ben-Shaul A, Nicholls A, Honig BH (1996) Free energy determinants of α-helix insertion into lipid bilayers. Biophys J 70: 1803

Bernèche S, Nina M, Roux B (1998) Molecular dynamics simulation of melittin in a dimyristoylphosphatidylcholine bilayer membrane. Biophys J 75: 1603

Bhattacharyya DK, Lecomte M, Rieke CJ, Garavito M, Smith WL (1996) Involvement of Arg 120, Glu 524 and Tyr 355 in the binding of arachidonate and 2-phenylpropionic acid inhibitors to the cyclooxygenase active site of ovine prostaglandin endoperoxidase H synthase-1. J Biol Chem 271: 2179

Boresch S, Archontis G, Karplus M (1994) Free energy simulations – the meaning of the individual contributions from a component analysis. Proteins 20: 25

Brooks BR, Bruccoleri RE, Olafson BD, States DJ, Swaminathan S, Karplus M (1983) Charmm: a program for macromolecular energy minimization and dynamics calculations. J Comput Chem 4: 187

Brunger AT, Karplus M (1988) Polar hydrogen positions in proteins: empirical energy placement and neutron diffraction comparison. Proteins 4: 148

Cowan SW, Schirmer T, Rummel G, Steiert M, Ghosh R, Pauptit RA, Jansonius TN, Rosenbusch JP (1992) Crystal structures explain functional properties of two *E. coli* porins. Nature 358: 727

Cowan SW, Garavito RM, Jansonius JN, Jenkins JA, Karlsson R, Konig N, Pai EF, Pauptit RA, Rizkallah PJ, Rosenbusch JP et al. (1995) The structure of OmpF porin in a tetragonal crystal form. The structure of OmpF porin in a tetragonal crystal form. Structure 3: 1041

Deisenhofer J, Michel H (1989) The photosynthetic reaction center from the purple bacterium rhodopseudomonas viridis. Science 245: 1463

Doyle DA, Cabral J, Morais Pfuetzner RA, Kuo A, Gulbis JM, Cohen SL, Chait BT, MacKinnon R (1998) The structure of the potassium channel: molecular basis of K^+ conduction and selectivity. Science 280: 69

Edholm O, Jahnig F (1988) The structure of a membrane-spanning polypeptide studied by molecular dynamics. Biophys Chem 30: 279

Eisenberg D, McLachlan AD (1986) Solvation energy in protein folding and binding. Nature 319: 199

Eisenberg D, Weiss RM, Terwilliger TC (1982) The helical hydrophobicity moment: a measure of the amphiphilicity of a helix. Nature 299: 371

Gennis RB (1989) Biomembranes: molecular structure and function. Springer, Berlin Heidelberg New York

Gilson MK, Honig B (1988) Energetics of charge-charge interactions in proteins. Proteins 3: 32

Henderson R, Baldwin JM, Ceska TA, Zemlin F, Beckmann E, Downing KH (1990) Model for the structure of bacteriorhodopsin based on high-resolution electron cryo-microscopy. J Mol Biol 213: 899

Hermann RB (1972) Theory of hydrophobic bonding. ii. the correlation of hydrocarbon solubility in water with solvent cavity surface area. J Phys Chem 76: 2754

Hla T, Ristimaki A, Appleby S, Barriocanal JG (1993) Cyclooxygenase gene expression in inflammation and angiogenesis. Ann NY Acad Sci 696: 197

Holtzman MJ, Turk J, Shornick LP (1991) Identification of a pharmacologically distinct prostaglandin H synthase in cultured epithelial cells. J Biol Chem 267: 21438

Honig B, Nicholls A (1995) Classical electrostatics in biology and chemistry. Science 268: 1144

Honig B, Sharp K, Yang A-S (1993) Macroscopic models of aqueous solutions: biological and chemical applications. J Phys Chem 97: 1101

Jacobs RE, White SH (1989) The nature of the hydrophobic binding of small peptides at the bilayer interface: implications for the insertion of transbilayer helices. Biochemistry 28: 3421

Jorgensen WL, Chandrasekhar J, Madura JD, Impey RW, Klein ML (1983) Comparison of simple potential functions for simulating liquid water. J Chem Phys 79: 926

Kaiser ET, Kezdy FJ (1987) Peptides with affinity for membranes. Annu Rev Biophys Biophys Chem 16: 561

Klapper I, Hagstrom R, Fine R, Sharp K, Honig B (1986) Focusing of electric fields in the active site of Cu-Zn superoxide dismutase: effects of ionic strength and amino-acid modification. Proteins 1: 47

Kurumbail RG, Stevens AM, Gierse JK, McDonald JJ, Stegeman RA, Pak JY, Gildehaus DD, Miyashiro JM, Penning TD, Seibert K, Isakson PC, Stallings WC (1996) Structural basis for selective inhibition of cyclooxygenase-2 by anti-inflammatory agents. Nature 384: 644

Loll OJ, Garavito RM (1994) The isoforms of cyclooxygenase structure and function. Exp Opin Invest Drugs 3: 1171

Loll PJ, Picot D, Garavito RM (1995) The structural basis of aspirin activity inferred from the crystal structure of inactivated prostaglandin H2 synthase. Nat Struct Biol 2: 637

Loll PJ, Picot D, Ekabo O, Garavito RM (1996) Synthesis and use of iodinated nonsteroidal antiinflammatory drug analogs as crystallographic probes of the prostaglandin H2 synthase cyclooxygenase active site. Biochemistry 35: 7330

Loof HD, Harvey SC, Segrest JP, Pastor RW (1991) Mean field stochastic boundary molecular dynamics simulation of a phospholipid in a membrane. Biochemistry 30: 2099

Luong C, Miller A, Barnett J, Chow J, Ramasha C, Browner M (1996) Flexibility of the NSAID binding site in the structure of human cyclooxygenase-2. Nat Struct Biol 3: 927

Mackerell AD Jr, Bashford D, Bellot M, Dunbrack RL, Field MJ, Fischer S, Gao J, Guo H, Joseph D, Ha S, Kuchnir L, Kuczera K, Lau FTK, Mattos C, Michnick S, Nguyen DT, Ngo T, Prodhom B, Roux B, Schlenkrich B, Smith J, Stote R, Straub J, Wiorkiewicz-Kuczera J, Karplus M (1998) All-atom empirical potential for molecular modeling and dynamics studies of proteins. J Phys Chem B 102: 3586

Mancini JA, Riendeau D, Falgueyret J-P, Vickers PJ, O'Neill GP (1995) Arginine 120 of prostaglandin G/H synthase-1 is required for the inhibition by nonsteroidal anti-inflammatory drugs containing a carboxylic acid moiety. J Biol Chem 270: 29372

Marrink S-J, Berendsen HJC (1994) Simulation of water transport through a lipid membrane. J Phys Chem 98: 4155

McCartney SA, Mitchell JA, Fairclough PD, Farthing MJ, Warner TD (1999) Selective COX-2 inhibitors and human inflammatory bowel disease. Aliment Pharmacol Ther 8: 1115

Meade EA, Smith WL, DeWitt DL (1993) Differential inhibition of prostaglandin endoperoxide synthase (cyclooxygenase) isozymes by aspirin and other non-steroidal anti-inflammatory drugs. J Biol Chem 268: 6610

Mendelsohn R, Davies MA, Brauner JW, Schuster HF, Dluhy RA (1989) Quantitative determination of conformational disorder in the acyl chains of phospholipid bilayers by infrared spectroscopy. Biochemistry 28: 8934–8939

Milik M, Skolnick J (1993) Insertion of peptide chains into lipid membranes: an off-lattice monte carlo dynamics model. Protein Struct Funct Genet 15: 10

Nagle JF (1993) Area/lipid of bilayer from NMR. Biophys J 64: 1476

Nina M, Beglov D, Roux B (1997) Atomic radii for continuum electrostatics calculations based on molecular dynamics free energy simulations. J Phys Chem 101: 5239

Ohki S, Ogino N, Yamamoto S, Hayaishi O (1979) Prostaglandin hydroperoxidase, an integral part of prostaglandin endoperoxide synthetase from bovine vesicular gland microsomes. J Biol Chem 254: 829

Otto JC, DeWitt DL, Smith WL (1993) N-glycosylation of prostaglandin endoperoxide synthases-1 and -2 and their orientations in the endoplasmic reticulum. J Biol Chem 268: 18234

Pagels WR, Sachs RJ, Marnett LJ, Dewitt DL, Day JS, Smith WL (1983) Immunochemical evidence for the involvement of prostaglandin H synthase in hydroperoxide-dependent oxidations by ram seminal vesicle microsomes. J Biol Chem 258: 6517

Pastor RW, Feller SE (1996) Time scales of lipids dynamics and molecular dynamics. In: Merz KM, Roux B (eds) Biological membranes. A molecular perspective from computation and experiment. Birkhauser, Boston, pp 3–29

Pastor RW, Venable RM, Karplus M (1991) Model for the structure of the lipid bilayer. Proc Natl Acad Sci USA 88: 892

Perozo E, Cortes DM, Cuello LG (1999) Structural rearrangements underlying K^+-channel activation gating. Science 285: 73–78

Philippsen A (1999) DINO: visualizing structural biology. http://www.bioz.unibas.ch/xray/dino

Picot D, Loll PJ, Garavito RM (1994) The X-ray crystal structure of the membrane protein prostaglandin H2 synthase-1. Nature 367: 243

Rieke CJ, Mulichak AM, Garavito RM, Smith WL (1999) The role of arginine 120 of human prostaglandin endoperoxide H synthase-2 in the interaction with fatty acid substrates and inhibitors. J Biol Chem 274: 17109

Roux B, Woolf TB (1996) Molecular dynamics of pf1 coat protein in a phospholipid bilayer. In: Merz KM, Roux B (eds) Biological membranes. A molecular perspective from computation and experiment. Birkhauser, Boston, pp 555–587

Ryckaert JP, Ciccotti G, Berendsen HJC (1977) Numerical integration of the cartesian equations of motion of a system with constraints: molecular dynamics of n-alkanes. J Comput Phys 23: 327

Sanner MF, Olson AJ, Spehner J-C (1995) Fast and robust computation of molecular surfaces. In: Proceedings of the 11th ACM symposium on computational geometry. ACM Press, Washington D.C., pp C6–C7

Schlenkrich MJ, Brickmann J Jr, Mackerell AD Jr, Karplus M (1996) An empirical potential energy function for phospholipids: criteria for parameters optimization and applications. In: Merz KM, Roux B (eds) Biological membranes. A molecular perspective from computation and experiment. Birkhauser, Boston, pp 31–81

Smith WL, Borgeat P, Fitzpatrick FA (1991) Biochemistry of lipids, lipoproteins and membranes. Elsevier, Amsterdam, p 297

Smith WL, Marnett LJ (1991) Prostaglandin endoperoxide synthase: structure and catalysis. Biochim Biophys Acta 1083: 1

Spencer AG, Thuresson E, Otto JC, Song I, Smith T, DeWitt DL, Garavito RM, Smith WL (1999) The membrane binding domains of prostaglandin endoperoxide H synthases 1 and 2. Peptide mapping and mutational analysis. J Biol Chem 274: 32936

van der Ouderaa FJ, Buytenhek M, Nugteren DH, van Dorp DA (1977) Purification and characterisation of prostaglandin endoperoxide synthetase from sheep vesicular glands. Biochim Biophys Acta 487: 315

Venable RM, Zhang Y, Hardy BJ, Pastor RW (1993) Molecular dynamics simulations of a lipid bilayer and of hexadecane: an investigation of membrane fluidity. Science 262: 223

Warwicker J, Watson HC (1982) Calculation of the electric potential in the active site cleft due to alpha-helix dipoles. J Mol Biol 157: 671

Wendt KU, Lenhart A, Schulz GE (1999) The structure of the membrane protein squalene-hopene cyclase at 2.0 Å resolution. J Mol Biol 286: 175

Wendt KU, Poralla K, Schulz GE (1997) Structure and function of a squalene cyclase. Science 277: 1811

White SH, Wiener MC (1996) The liquid crystallographic structure of fluid lipid bilayer membranes. In: Merz KM, Roux B (eds) Biological membranes. A molecular perspective from computation and experiment. Birkhauser, Boston, pp 127–144

Woolf TB, Roux B (1994) The conformational flexibility of *O*-phosphorylcholine and *O*-phosphorylethanolamine: a molecular dynamics study of solvation effects. J Am Chem Soc 116: 5916

Woolf T, Roux B (1996) Structure, energetics and dynamics of lipid-protein interactions: a molecular dynamics study of the gramicidin A channel in a DMPC bilayer. Proteins Struct Funct Genet 24: 92

Yi L, Grabski S, DeWitt DL (1998) The membrane association sequences of the prostaglandin endoperoxide synthases-1 and -2 isozymes. J Biol Chem 273: 29830